

FIRST-PRINCIPLES MODELING OF BIPOLAR RESISTIVE SWITCHING IN METAL-OXIDE BASED MEMORY

Alexander Makarov, Josef Weinbub, Viktor Sverdlov, and Siegfried Selberherr

Institute for Microelectronics
Technische Universität Wien
Gusshausstrasse 27–29
1040 Vienna, Austria

Email: {makarov|weinbub|sverdlov|selberherr}@iue.tuwien.ac.at

KEYWORDS

RRAM, resistive switching mechanism, stochastic model, Monte Carlo method

ABSTRACT

A microscopic model of the resistive switching mechanism in bipolar metal-oxide based resistive random access memory (RRAM) is presented. The distribution of electron occupation probabilities obtained is in agreement with previous work. In particular, a low occupation region is formed near the cathode. A hysteresis cycle of RRAM switching simulated with the model including the ion dynamics is in good agreement with experimental results.

INTRODUCTION

The resistive switching phenomenon is observed in different types of insulators, such as metal oxides, perovskite oxides, and chalcogenide materials. Because the electrical conductance of the insulator can be set at different levels by the application of an electric field, this phenomenon becomes attractive for advanced memory concepts. Indeed, a state with high resistance can be interpreted as logical 1 and a state with low resistance as logical 0, or vice versa, depending on the technology. The concepts of memory using the resistive switching phenomenon can be conveniently divided into the following three categories: Conductive Bridge RAM (CBRAM), Phase Change RAM (PCRAM), and Resistive RAM (RRAM). CBRAM is based on a solid-state electrolyte in which mobile metal ions create a conductive bridge between the two electrodes under the influence of an electric field. PCRAM employs the difference in resistivity between the crystalline and amorphous phases of a chalcogenide compound. RRAM is based on metal oxides, such as TiO_x (Kugeler et al. 2008), HfO_2 (Chen et al. 2009), Cu_xO (Dong et al. 2007), NiO (Seo et al. 2005), ZnO (Lee et al. 2009) and perovskite oxides, such as doped SrTiO_3 (Watanabe et al.

2001), doped SrZrO_3 (Lin et al. 2007), $\text{Pr}_{1-x}\text{Ca}_x\text{MnO}_3$ (Sawa et al. 2004), and employs the electric field induced difference in resistivity between the high and low current carrying states.

The increasing demand for miniaturization of microelectronic devices has significantly accelerated the search for new concepts of nonvolatile memory during the last few years. Memory based on charge storage (such as flash memory, and others) is gradually approaching the physical limits of scalability, and conceptually new types of memories based on a different storage principle are gaining momentum. Apart from good scalability, a new type of memory must also exhibit low operating voltages, low power consumption, high operation speed, long retention time, high endurance, and simple structure (Lee et al. 2010 ; Kryder and Kim 2009).

In addition to RRAM, PCRAM, and CBRAM there exist several other concepts as potential replacements of the charge memory. Some of the technologies are already available in prototype form (such as carbon nanotube RAM (NRAM)), others as product (magnetoresistive RAM (MRAM), ferroelectric RAM (FRAM)), while the technologies of spin-torque transfer RAM (STTRAM) and racetrack memory are under intensive research.

From these concepts the CBRAM, PCRAM, and RRAM possess the simplest metal-insulator-metal (MIM) structure and, as a consequence, have good scalability. This fact gives advantages to RRAM, PCRAM, and CBRAM over other advanced memory concepts.

In addition to its simple structure RRAM is characterized by a low operating voltage (< 2 V), fast switching time (< 10 ns), high density, and long retention time. Several physical mechanisms based on either electron or ion switching have been recently suggested in the literature: a model based on trapping of charge carriers (Fujii et al. 2005), electrochemical migration of oxygen vacancies (Nian et al. 2007; Wu et al. 2008), electrochemical migration of oxygen ions (Szot et al. 2006; Nishi et al. 2008), a unified physical model (Gao et al. 2009), a domain model (Rozenberg et al. 2004), a filament anodization model (Kinoshita et al. 2006), a thermal dissolution model (Russo et al. 2007), a two-variable

resistor model (Kim and Choi 2009), and others. Despite these efforts, however, a proper fundamental understanding of the RRAM switching mechanism is still missing, hindering further development of this type of memory.

We propose a stochastic model of the resistive switching mechanism based on electron hopping between the oxygen vacancies along the conductive filament in an oxide-layer, where a redox reaction plays a crucial role in the resistive switching from the state with low resistance to the state with high resistance and back.

MODEL DESCRIPTION

We associate the resistive switching behavior in the oxide-based memory with the formation and rupture of a conductive filament (CF). The CF is formed by localized oxygen vacancies (V_o) (Gao et al. 2009) or domains of V_o . Formation and rupture of a CF is due to a redox reaction in the oxide layer under a voltage bias. The conduction is due to electron hopping between these V_o . (Fig. 1)

For modeling the resistive switching in oxide-based memory by Monte Carlo techniques, we describe the dynamics of oxygen ions (O^{2-}) and electrons in an oxide layer as follows:

- formation of V_o by O^{2-} moving to an interstitial position;
- annihilation of V_o by moving O^{2-} to V_o ;
- an electron hop on V_o from an electrode;
- an electron hop out from V_o to an electrode;
- an electron hop between two V_o .

In order to model the dependence of transport on the applied voltage and temperature we choose the hopping rates as (Sverdlov et al. 2001):

$$\Gamma_{nm} = A_e \cdot \frac{dE}{1 - \exp(-dE/T)} \cdot \exp(-R_{nm}/a). \quad (1)$$

Here, A_e is a coefficient, $dE = E_n - E_m$ is the difference between the energies of an electron positioned at the sites n and m , R_{nm} is the hopping distance, a is the localization radius. The hopping rates between an electrode (0 or $N + 1$) and an oxygen vacancy m are described by:

$$\Gamma_m^{iC} = 2 \cdot \alpha \cdot f \cdot \Gamma_{0m}, \Gamma_m^{oC} = 2 \cdot \alpha \cdot (1 - f) \cdot \Gamma_{m0}, \quad (2)$$

$$\Gamma_m^{iA} = 2 \cdot \beta \cdot f \cdot \Gamma_{(N+1)m}, \Gamma_m^{oA} = 2 \cdot \beta \cdot (1 - f) \cdot \Gamma_{m(N+1)}. \quad (3)$$

Here, f is the electrode occupation probability, α and β are the coefficients of the boundary conditions on the

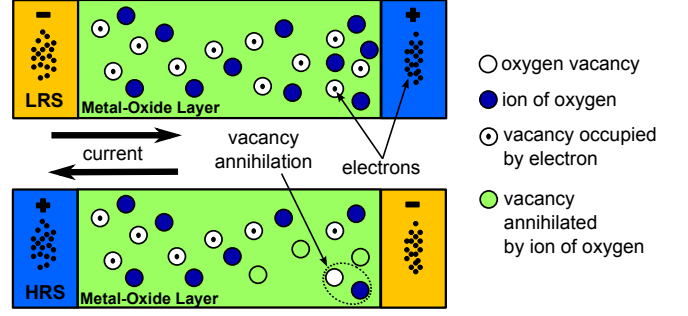


Figure 1: A schematic illustration of the conducting filament in the low resistance state (top) and the high resistance state (bottom).

cathode and anode, respectively, N is the number of sites, A and C stand for cathode and anode, and i and o for hopping on the site and out from the site, respectively.

To describe the motion of ions we have chosen the ion rates similar to (1):

$$\Gamma'_n = A_i \cdot \frac{dE}{1 - \exp(-dE/T)}. \quad (4)$$

Here we assume that O^{2-} can only move to the nearest interstitial, and a distance-dependent term is thus included in A_i . dE includes the formation energy for the n^{th} V_o /annihilation energy of the n^{th} V_o , when O^{2-} is moving to an interstitial or back to V_o , respectively.

The electron current generated by hopping is calculated as:

$$I = q_e \cdot \sum dx / \sum \left(1 / \sum_m \Gamma_m \right). \quad (5)$$

SIMULATION TOOL

For modeling the RRAM switching behavior a simulation tool was developed which allows simulating 1D/2D/3D model systems. C++ was chosen as programming language. Fig. 2 shows a flow chart of the simulation process performed by the tool.

The module "starter" is a basic module which allows choosing different modes of simulation to produce results for a particular experiment of interest.

In the module "random generator" a random number generator using the l'Ecuyer algorithm (Press et al. 1992) was implemented. This algorithm allows random number generation with a practically infinite period ($\sim 2 \times 10^{18}$).

The dimension (1D/2D/3D), size, site location, site energies, and other parameters describing the structure under the simulation are defined in the module "description of elements".

The input parameters are set in an initialization file as shown:

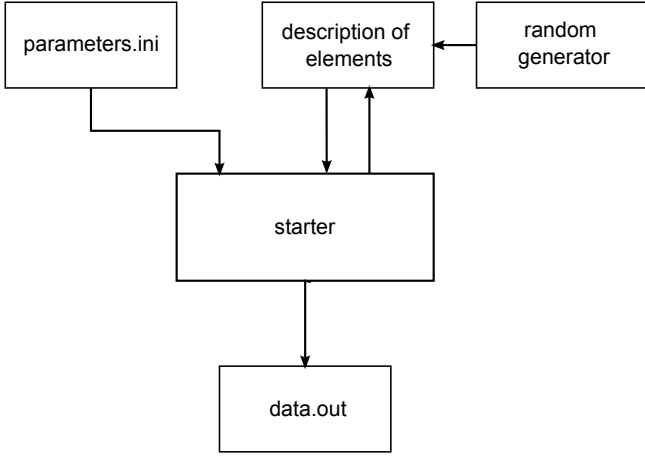


Figure 2: Basic schema of modules of the simulation tool.

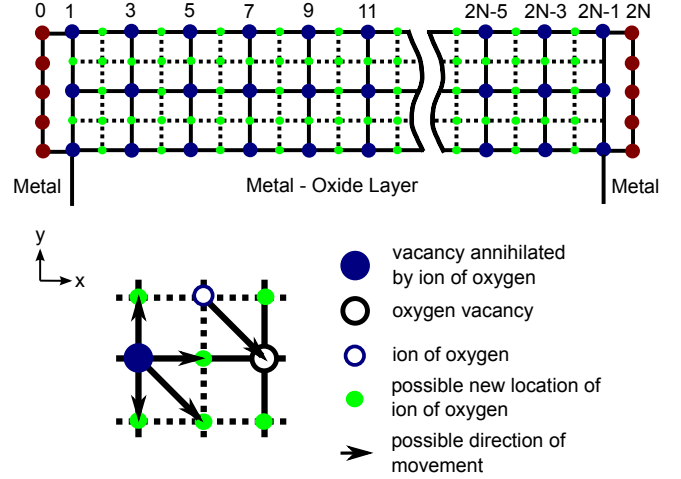


Figure 3: A schematic picture of the unit cell of the model system.

```

1 [Experiment]
2 type=2
3 n=1
4 [Lattice]
5 x=30
6 y=10
7 z=1
8 def=0
9 [RedoxEnergy]
10 E0=0.036
11 E1=5.0
12 E2=0.018
13 E3=0.036
14 E4=5.0
15 E5=0.018
16 [Stochastic]
17 Ae=100000
18 a=2
19 Ai=100
20 eR=25
21 iR=1
22 [Environmental]
23 T=0.025
24 [Set]
25 U=1.3
26 t=0.0
27 alpha=0.1
28 beta=0.1
29 f=0.5
30 [Reset]
31 U=-1.0
32 t=0.0
33 alpha=0.1
34 beta=0.1
35 f=0.5
36 [Change]
37 dU=0.01
38 dt1=0.01
39 dt2=0.001
40 dt3=0.01
41 dt4=0.001
  
```

Fig.3 demonstrates an example of a unit cell for a two-dimensional array of sites. The columns with number 0 and $2N$ are reserved for the electrodes (anode and cathode). By moving O^{2-} from a lattice site to an interstitial a vacancy V_o at the lattice site is formed. In the first moment of time we assume that there are no vacancies V_o . Each O^{2-} has a probability Γ'_n of moving to the nearest interstitial position (if this position is empty) making a formation of a new V_o possible; moreover, each O^{2-} has a probability Γ'_n of annihilation with the nearest V_o if this V_o is not occupied by an electron. In addition, the electron dynamics according to (1-3) on the vacancies V_o already formed must also be taken into account giving rise to the electron current in the system.

MODEL VERIFICATION

All calculations are made on one or/and two-dimensional lattices, the distances between two nearest neighboring V_o in all directions are equal. All V_o are at the same energy level, if no voltage or temperature is applied. Despite the fact that in the binary metal oxides V_o can have three different charge states with charge 0, +1, +2 (Schmidt-Mende and MacManus-Driscoll 2007), to simplify the calculations, we assume that the V_o is either empty or occupied by one electron. This assumption is not a limitation, however, due to the energy separation between the three charge states only two of them will be relevant for hopping and significantly contribute to transport.

Calculation of electron occupation probability

In order to verify the proposed model and our implementation in a simulation tool, we first evaluate the average electron occupations of hopping sites under different conditions. For comparison with previous works all calculations in this subsection are made on a one-dimensional lattice consisting of thirty equivalent, equidistantly positioned hopping sites V_o .

To implement all the above conditions, we used a model system with the artificially inflated value for annihilation energy of V_o , low value of formation energy for V_o , and large A_i . The low value of formation energy for V_o is used to guarantee that all O^{2-} are moved to the interstitial positions. An increased value for the annihilation energy of V_o is used guaranteeing that the already formed V_o will not be annihilated by O^{2-} .

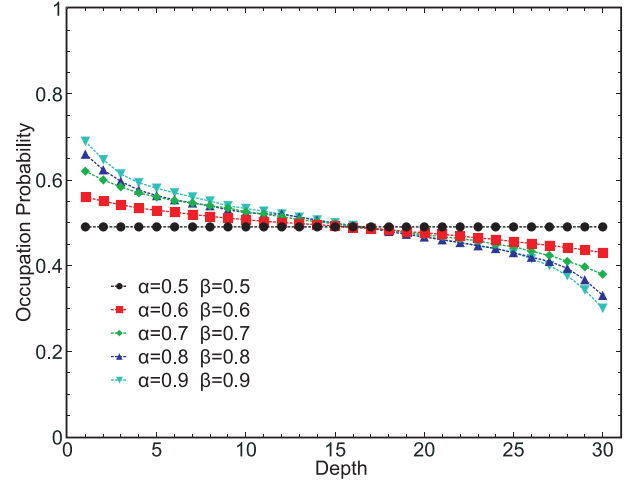
Large values A_i are needed for accelerating the process of the CF formation. In order to compare our results with (Derrida 1998), we use for the occupation probability $f = 0.5$.

Following (Derrida 1998), we first allow hopping in one direction and only to/from the closest V_o (asymmetric single exclusion process).

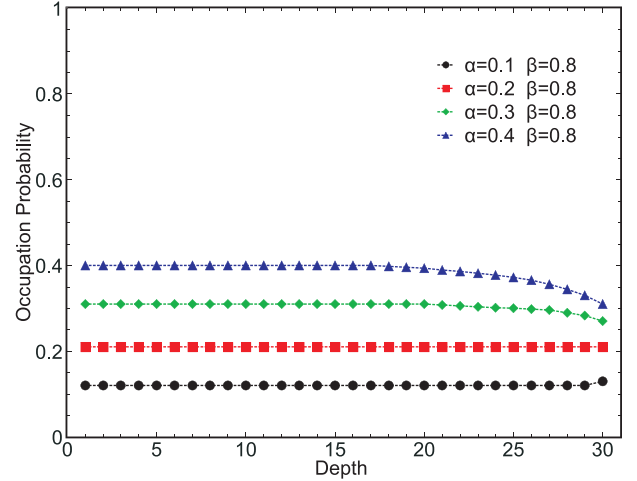
Each site i of a one-dimensional lattice of N sites is either occupied by an electron or empty; during a time interval dt , each electron has a probability Γ_{nm} of hopping to the right, provided the target site is empty; moreover, during the time interval dt , an electron may enter the lattice at the Site 1 with the probability $\alpha \cdot \Gamma_{01}$ (if this site is empty) and an electron at the Site N may leave the lattice with the probability $\beta \cdot \Gamma_{N(N+1)}$ (if this site is occupied). The occupation probability p_c of a central V_o (p_c) is described, depending on the boundary conditions, as follows: 1) for $\alpha > 0.5$ and $\beta > 0.5$, $p_c = 0.5$; 2) for $\alpha < 0.5$ and $\alpha < \beta$, $p_c = \alpha$ 3) for $\beta < 0.5$ and $\beta < \alpha$, $p_c = 1 - \beta$. Fig.4 shows simulation results of the stochastic model, which fully obey the theoretical calculations (Derrida 1998).

To move from a model system of an asymmetric single exclusion process (Derrida 1998) to a more realistic structure, we have demonstrated the dependence of electron occupation probabilities from the position of the Fermi level in the electrodes relative to the energy level of the sites, determined by the value of f . Fig. 5 shows the result of our simulations.

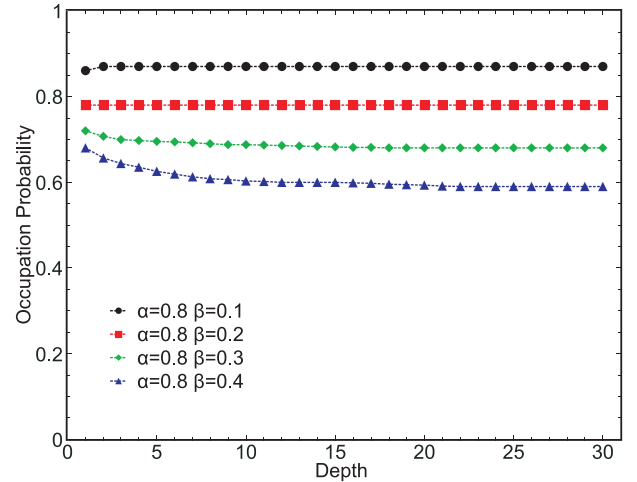
We have further calibrated the model in a manner to reproduce the results reported in (Gao et al. 2009), for $V = 0.6V$ to $V = 1.4V$. Fig.6 shows a case, when the hopping rate between the two V_o is larger than the rate between the electrodes and V_o (i.e. $\alpha, \beta < 1$). In this case a low occupation region is formed near the cathode (bipolar behavior).



(a)

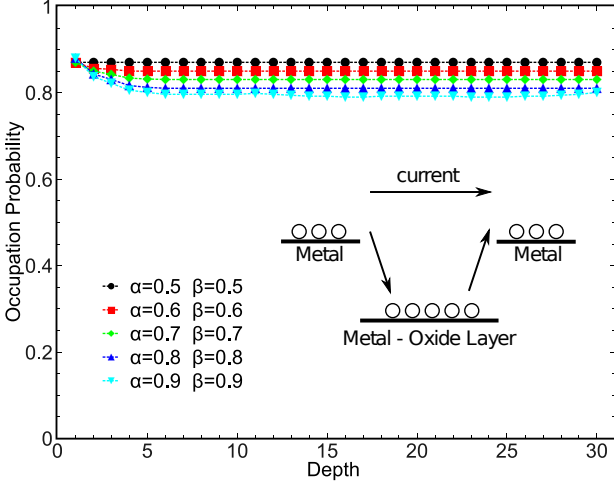


(b)

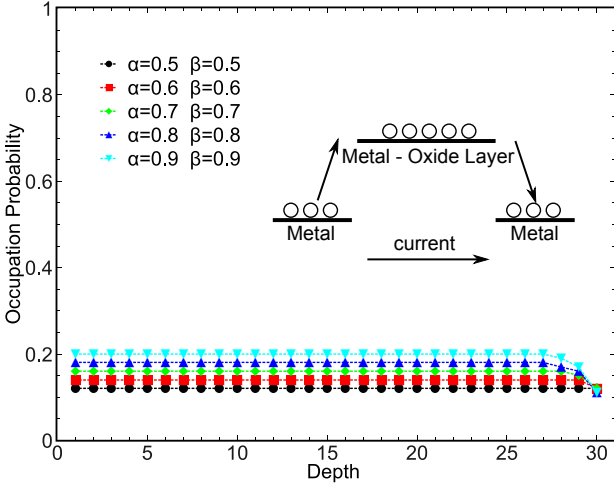


(c)

Figure 4: Calculated distribution of electron occupation probabilities for unidirectional next nearest neighbor hopping between the V_o (the 1st V_o is near the cathode, the last V_o is near the anode): (a) $\alpha > 0.5$ and $\beta > 0.5$, $p_c = 0.5$; (b) $\alpha < 0.5$ and $\alpha < \beta$, $p_c = \alpha$; (c) $\beta < 0.5$ and $\beta < \alpha$, $p_c = 1 - \beta$.



(a)



(b)

Figure 5: Calculated distribution of electron occupation probabilities for unidirectional next nearest neighbor hopping between the V_o $\alpha > 0.5$ and $\beta > 0.5$: (a) $f = 0.9$; (b) $f = 0.1$.

Modeling of the hysteresis cycle

All calculations of the RRAM $I - V$ characteristics are now performed on a two-dimensional lattice (10×30). We have investigated the $I - V$ hysteresis by applying a saw-tooth-like voltage V . We have assumed that the coefficients α and β of the boundary conditions are constant and equal to 0.1.

The simulated RRAM switching hysteresis cycle is shown in Fig. 7. The simulated cycle is in good agreement with the experimental cycle from (Lee et al. 2009) shown in the inset to Fig. 7.

The interpretation of the RRAM hysteresis cycle obtained from the microscopic model is as follows. If a positive voltage is applied, the formation of a CF begins, when the voltage reaches a critical value sufficient to create V_o by moving O^{2-} to an interstitial position. The formation of the CF leads to a sharp increase in

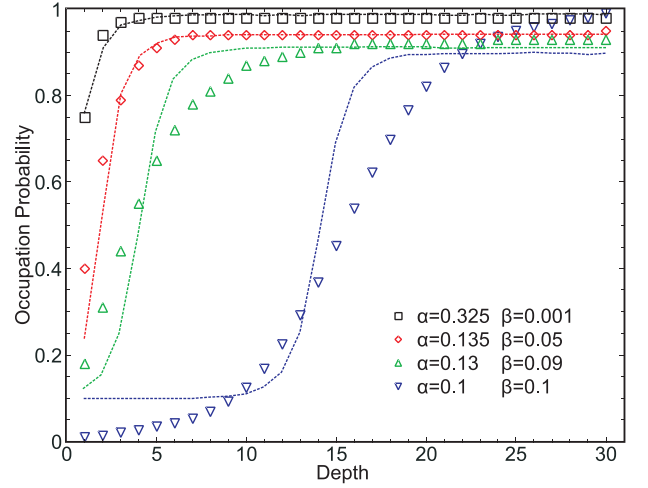


Figure 6: Calculated distribution of electron occupation probabilities under different biasing voltages. Lines are from (Gao et al. 2009), symbols are obtained from our model.

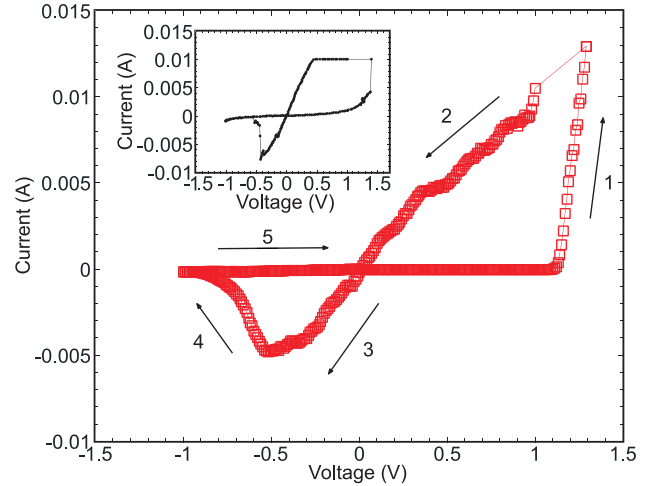


Figure 7: $I - V$ characteristics showing the hysteresis cycle obtained from our model ($\alpha = 0.1$ and $\beta = 0.1$). The inset shows the hysteresis cycle for $M - \text{ZnO} - M$ from (Lee et al. 2009).

the current (Fig. 7, Segment 1) signifying a transition to a state with low resistance. When a reverse negative voltage is applied, the current flows in a different direction and first increases linearly in voltage (Fig. 7, Segment 3), until the applied voltage reaches the value at which an annihilation of V_o is triggered by means of moving O^{2-} to V_o . The CF is ruptured and the current decreases (Fig. 7, Segment 4). This is the transition to a state with high resistance.

CONCLUSION

In this work we have presented a microscopic model of the bipolar resistive switching mechanism. The distribution of the electron occupation probabilities calculated with the model is in excellent agreement with previous work. The simulated RRAM switching hysteresis cycle is in good agreement with the experimental result. The proposed microscopic model can be used for performance optimization of RRAM devices.

ACKNOWLEDGMENTS

This research is supported by the European Research Council through the grant #247056 MOSILSPIN.

REFERENCES

- Chen, Y.S.;** T.Y. Wu; P.J. Tzeng. 2009. "Forming-free HfO₂ Bipolar RRAM Device with Improved Endurance and High Speed Operation." *Symp. on VLSI Tech.*, 37-38.
- Derrida, B.** 1998. "An Exactly Soluble Non-Equilibrium System: The Asymmetric Simple Exclusion Process." *Phys. Rep.*, vol. 301, no. 1-3, 65-83.
- Dong, R.;** D.S. Lee; W.F. Xiang; S.J. Oh; D.J. Seong; S.H. Heo. 2007. "Reproducible Hysteresis and Resistive Switching in Metal-Cu_xO-Metal Heterostructures." *Appl. Phys. Lett.*, vol. 90, no. 4, 42107/1-3.
- Fujii, T.;** M. Kawasaki; A. Sawa; H. Akoh; Y. Kawazoe; Y. Tokura. 2005. "Hysteretic Current-Voltage Characteristics and Resistance Switching at an Epitaxial Oxide Schottky Junction SrRuO₃/SrTi_{0.99}Nb_{0.01}O₃." *Appl. Phys. Lett.*, vol. 86, no. 1, art. no. 012107.
- Gao, B.;** B. Sun; H. Zhang; L. Liu; X. Liu; R. Han; J. Kang; B. Yu. 2009. "Unified Physical Model of Bipolar Oxide-Based Resistive Switching Memory." *IEEE Electron Device Lett.*, vol. 30, no. 12, 1326-1328.
- Kim, S.;** Y.K. Choi. 2009. "A Comprehensive Study of the Resistive Switching Mechanism in Al/TiO_x/TiO₂/Al-Structured RRAM." *IEEE Trans. Electron Devices*, vol. 56, no. 12, pp. 3049-3054.
- Kinoshita, K.;** T. Tamura; H. Aso; H. Noshiro; C. Yoshida; M. Aoki; Y. Sugiyama; H. Tanaka. 2006. "New Model Proposed for Switching Mechanism of ReRAM." *IEEE Non-Volatile Semicond. Memory Workshop*, 84-85.
- Kryder, M.H.;** C.S. Kim. 2009. "After Hard Drives - What Comes Next?" *IEEE Trans. Magn.*, vol. 45, no. 10, 3406-3413.
- Kugeler C.;** C. Nauenheim; M. Meier; A. Rudiger; R. Waser. 2008. "Fast resistance switching of TiO₂ and MSQ thin films for nonvolatile memory applications (RRAM)." *NVM Tech. Symp.*, 6.
- Lee, S.;** H. Kim; D.J. Yun; S.W. Rhee; K. Yong. 2009. "Resistive Switching Characteristics of ZnO Thin Film Grown on Stainless Steel for Flexible Nonvolatile Memory Device." *Appl. Phys. Lett.*, vol. 95, no. 26, 262113.
- Lee, B.C.;** P. Zhou; J. Yang; Y.T. Zhang; B. Zhao; E. Ipek; O. Mutlu; D. Burger. 2010. "Phase-Change Technology and the Future of Main Memory." *IEEE Micro*, vol. 30, no. 1, 131-141.
- Lin, C.C.;** C.Y. Lin; M.H. Lin. 2007. "Voltage-Polarity-Independent and High-Speed Resistive Switching Properties of V-Doped SrZrO₃ Thin Films." *IEEE Trans. Electron Devices*, vol. 54, no. 12, 3146-3151.
- Nian, Y.B.;** J. Strozier; N.J. Wu; X. Chen; A. Ignatiev. 2007. "Evidence for an Oxygen Diffusion Model for the Electric Pulse Induced Resistance Change Effect in Transition-Metal Oxides." *Phys. Rev. Lett.*, vol. 98, no. 14, 146403/1-4.
- Nishi, Y.;** J.R. Jameson. 2008. "Recent Progress in Resistance Change Memory." *Dev. Res. Conf.*, 271-274.
- Press, W.H.;** S.A. Teukolsky; W.T. Vetterling; B.P. Flannery. 1992. "Numerical Recipes in C: the art of scientific computing." *Cambridge University Press*.
- Rozenberg, M.J.;** I.H. Inoue; M.J. Sanchez. 2004. "Nonvolatile Memory with Multilevel Switching: A Basic Model." *Phys. Rev. Lett.*, vol. 92, no. 17, 178302-1.
- Russo, U.;** D. Ielmini; C. Cagli; A.L. Lacaita; S. Spiga; C. Wiemer; M. Perego; M. Fanciulli. 2007. "Conductive-Filament Switching Analysis and Self-Accelerated Thermal Dissolution Model for Reset in NiO-Based RRAM." *IEDM Tech. Dig.*, 775-778.
- Sawa, A.;** T. Fujii; M. Kawasaki; Y. Tokura. 2004. "Hysteretic Current-Voltage Characteristics and Resistance Switching at a Rectifying Ti/Pr_{0.7}Ca_{0.3}MnO₃ Interface." *Appl. Phys. Lett.*, vol. 85, no. 18, 4073-4075.
- Schmidt-Mende, L.;** J.L. MacManus-Driscoll. 2007. "ZnO - nanostructures, defects, and devices." *Materials today*, vol. 10, 40.
- Seo, S.;** M.J. Lee; D.H. Seo; S.K. Choi; D.S. Suh; Y.S. Joung; I.K. Yoo; I.S. Byun; I.R. Hwang; S.H. Kim; B.H. Park. 2005. "Conductivity Switching Characteristics and Reset Currents in NiO Films." *Appl. Phys. Lett.*, vol. 86, no. 9.
- Sverdlov, V.;** A.N. Korotkov; K.K. Likharev. 2001. "Shot-Noise Suppression at Two-Dimensional Hopping." *Phys. Rev. B*, vol. 63, 081302.
- Szot, K.;** W. Speier; G. Bihlmayer; R. Waser. 2006. "Switching the Electrical Resistance of Individual Dislocations in Single-Crystalline SrTiO₃." *Nature Materials*, vol. 5, 312-320.
- Watanabe, Y.;** J.G. Bednorz; A. Bietsch; Ch. Gerber; D. Widmer; A. Beck; S.J. Wind. 2001. "Current-Driven Insulator-Conductor Transition and Nonvolatile Memory in Chromium-Doped SrTiO₃ Single Crystals." *Appl. Phys. Lett.*, vol. 78, no. 23, 3738-3740.
- Wu, S.X.;** L.M. Xu; X.J. Xing. 2008. "Reverse-Bias-Induced Bipolar Resistance Switching in Pt/TiO₂/SrTi_{0.99}Nb_{0.01}O₃/Pt Devices." *Appl. Phys. Lett.*, vol. 93, no. 4, 043502/1-3.